Diffusion-Limited Size-Selective Ion Sensing Based on SAM-Supported Peptide Nanotubes

Kianoush Motesharei and M. Reza Ghadiri*

Contribution from the Departments of Chemistry & Molecular Biology and The Skaggs Institute for Chemical Biology, The Scripps Research Institute, La Jolla, California 92037

Received August 5, 1997[⊗]

Abstract: An approach for the construction of diffusion-limited size-selective sensors is described based on the self-assembly of cyclic peptides into tubular channels in organosulfur self-assembled monolayers on gold films. An eight-residue cyclic peptide of alternating units of D-Leu and L-Trp amino acid residues was incorporated into monolayers of dodecanethiol and octadecyl sulfide and shown to adopt highly oriented tubular structures under specified adsorption conditions. The structural properties of monolayer-supported peptide nanotubes have been analyzed by grazing angle FTIR spectroscopy and their selective ion transport activities by cyclic voltammetry and impedance spectroscopy.

Introduction

Contemporary biosensor devices are generally based on enzymatic catalysis or specific molecular recognition events mediated by the rich repertoire of antibodies and natural protein receptors.[1] Biosensors can be classified as either affinity[2] or dynamic[3] sensors. Affinity-based sensors are typically designed on the basis of immobilized and specific molecular recognition systems (such as antibodies and natural protein receptors) that are coupled to a signal transduction structure. While such devices can operate with high specificity, they necessarily do so by sacrificing turnover rates. Therefore, affinity type biosensors are often insensitive to time-dependent changes in analyte concentration and are often not useful in settings where rapid and multiple measurements are needed. On the other hand, dynamic sensors which depend often on adsorption or diffusional processes into nonspecific matrices can be used in rapid real-time sensing of analytes. In such systems, the sensing selectivity must be extracted from the differential response of sensor arrays, each configured for a particular response to a class of analytes.[3b,c,f] Here we describe our first steps toward the design of dynamic biosensors based on channel-mediated diffusional processes.

Formation of hollow tubular structures based on self-assembly of flat ring-shaped cyclic peptides has been well-documented,[4,5] and appropriately designed systems have also been shown to form transmembrane ion channels and pore structures.[6] In the present study we report the formation of oriented ion channels based on self-assembling peptide nanotubes in organosulfur monolayers on gold surfaces (Figure 1).

Self-assembled monolayers (SAMs) of organosulfurs on gold films[7] have been shown to form highly organized and ordered

[⊗] Abstract published in *Advance ACS Abstracts,* November 1, 1997.

(1) (a) Göpel, W.; Hesse, J.; Zemel, N. J.; Eds. *Sensors*; Wiley-VCH; Weinheim, 1989-1996; Vols. 1-8. (b) Scheller, F. W., Schubert, F., Ferrowitz, J., Eds. *Frontiers in Biosensorics*; Birkhäuser Verlag: Berlin, 1996; Vols. I and II. (c) Janata, J. *Principles of Chemical Sensors*; Plenum Press: New York, 1989. (d) Brecht, A.; Gauglitz, G. *Biosens. Bioelectron.* **1995**, *10*, 923. (e) Yim, H. S.; Kibbey, C. E.; Ma, S. C.; Kliza, D. M.; Liu, D.; Park, S. B.; Torre, C. E.; Meyerhoff, M. E. *Biosens. Bioelectron.* **1993**, *8*, 1.

(2) (a) Brecht, A.; Gauglitz, G. *Frontiers in Biosensorics II: Practical Applications*; Scheller, F. W., Schubert, F., Ferrowitz, J., Eds.; Birkhäuser: Verlag: Basel/Switzerland, 1997; pp 1−16. (b) ShriverLake, L. C.; Donner, B. L.; Ligler, F. S. *Environ. Sci., Technol.* **1997**, *31*, 837. (c) Piehler, J.; Brecht, A.; Gauglitz, G. *Anal. Chem.* **1996**, *68*, 139. (d) Wadkins, R. M.; Golden, J. P.; Ligler, F. S. *Anal. Biochem.* **1995**, *232*, 73. (e) Rabbany, S. Y.; Kusterbeck, A. W.; Bredehorst, R.; Ligler, F. S. *Sens. Actuators, B* **1995**, *29*, 72. (f) Kooyman, R. P. H.; van den Heuvel, D. J.; Drijfhout, J. W.; Welling, G. W. *Thin Solid Films* **1994**, *244*, 913. (g) van den Heuvel, D. J.; Kooyman, R. P. H.; Drijfhout, J. W.; Welling, G. W. *Anal. Biochem.* **1993**, *215*, 223. (h) Leckband, E. E.; Isrealachvili, J. N.; Schmitt, F.-J.; Knoll, W. *Science* **1992**, *255*, 1419. (i) Haussling, L.; Michel, B.; Ringsdorf, H.; Rohrer, H. *Angew. Chem., Int. Ed. Engl.* **1991**, *30*, 569. (j) Hickman, J. J.; Ofer, D.; Laibinis, P. E.; Whitesides, G. M.; Wrighton, M. S. *Science* **1991**, *252*, 688. (k) Ahlers, M.; Blankenburg, R.; Grainger, D. W.; Meller, P.; Ringsdorf, H.; Salesse, C. *Thin Solid Films* **1989**, *180*, 93.

(3) (a) Ferbuson, J. A.; Boles, T. C.; Walt, D. R. *Nat. Biotechnol.* **1996**, *14*, 1681. (b) Dickinson, T. A.; White, J.; Kauer, J. S.; Walt, D. R. *Nature* **1996**, *382*, 697. (c) White, J.; Kauer, J. S.; Dickinson, T. A.; Walt, D. R. *Anal. Chem.* **1996**, *68*, 2191. (d) Longergan, M. C.; Severin, E. J.; Doleman, B. J.; Grubbs, R. H.; Lewis, N. S. *Chem. Mater.* **1996**, *8*, 2298. (e) Henke, C.; Steinem, C.; Janshoff, A.; Steffan, G.; Luftmann, H.; Sieber, M.; Galla, H.-J. *Anal. Chem.* **1996**, *68*, 3158. (f) Freund, M. S.; Lewis, N. S. *Proc. Natl. Acad. Sci. U.S.A.* **1995**, *92*, 2652. (g) Bernard, A.; Bosshard, H. R. *Eur. J. Biochem.* **1995**, *230*, 416. (h) Lukosz, W. *Sens. Actuators, B* **1995**, *29*, 37. (i) Goddard, N. J.; Pollard-Knight, D.; Maule, C. H. *Analyst* **1994**, *119*, 583. (j) Odashima, K.; Kotato, M.; Sugarara, M.; Umezawa, Y. *Anal. Chem.* **1993**, *65*, 927. (k) Walt, D. R. *Chem. Ind. (London)* **1992**, 58. (l) Barnard, S. M.; Walt, D. R. *Nature* **1991**, *353*, 338. (m) Barnard, S. M.; Walt, D. R. *Science* **1991**, *251*, 4996. (n) Nagase, S.; Kataoka, M.; Naganawa, R.; Komatsu, R.; Odashima, K.; Umezawa, Y. *Anal. Chem.* **1990**, *62*, 1252. (o) Sugawara, M.; Kataoka, M.; Odashima, M.; Umezawa, Y. *Thin Solid Films* **1989**, *180*, 129. (p) Hafeman, D. G.; Parce, J. W.; McConnel, H. M. *Science (Washington, D.C.)* **1988**, *240*, 1182.

(4) (a) Ghadiri, M. R.; Granja, J. R.; Milligan, R. A.; McRee D. E.; Khazanovich, N. *Nature* **1993**, *366*, 324. (b) Khazanovich, N.; Granja, J. R.; McRee, D. E.; Milligan, R. A.; Ghadiri, M. R. *J. Am. Chem. Soc.* **1994**, *116*, 6011. (c) Ghadiri, M. R. *Adv. Mater.* **1995**, *7*, 675.

(5) (a) De Sanis, P.; Morosetti, S.; Rizzo, R. *Macromolecules* **1974**, *7*, 52. (b) Tomasic, L.; Lorenzi, G. P. *Helv. Chim. Acta* **1978**, *70*, 1012. (c) Pavone, V.; Benedetti, E.; Di Blasio, B.; Lombardi, A.; Pedone, C.; Tomasich, L.; Lorenzi, G. P. *Biopolymers* **1989**, *28*, 215. (d) Sun, X.; Lorenzi, G. P. *Helv. Chim. Acta* **1994**, *77*, 1520.

(6) (a) Ghadiri, M. R.; Granja, J. R.; Buehler, L. K. *Nature* **1994**, *369*, 301. (b) Granja, J. R.; Ghadiri, M. R. *J. Am. Chem. Soc.* **1994**, *116*, 10785. (c) Engels, M.; Bashford, D.; Ghadiri, M. R. *J. Am. Chem. Soc.* **1995**, *117*, 9151.

(7) For a general introduction to SAMs see: (a) Ulman, A. *Ultrathin Organic Films from Langmuir Blodgett to Self-Assembly*; Academic Press: New York, 1991. (b) Ulman, A., Ed. *Characterization of Organic Thin Films*; Butterworth-Heinemann: Boston, 1995. (c) Ulman, A. *Chem. Rev.* **1996**, *96*, 1533. (d) Nuzzo, R. G.; Allara, D. L. *J. Am. Chem. Soc.* **1983**, *105*, 4481. (e) Nuzzo, R. G.; Zegarski, B.; Dubois, L. H. *J. Am. Chem. Soc.* **1987**, *109*, 733. (f) Bain, C. D.; Whitesides, G. M. *Science* **1988**, *240*, 62. (g) Bain, C. D.; Whitesides, G. M. *J. Am. Chem. Soc.* **1988**, *110*, 3665. (h) Strong, L.; Whitesides, G. M. *Langmuir* **1988**, *4*, 546. (i) Bain, C. D.; Whitesides, G. M. *J. Am. Chem. Soc.* **1988**, *110*, 5897. (j) Troughton, E. B.; Bain, C. D.; Whitesides, G. M.; Nuzzo, R. G.; Allara, D. L.; Porter, M. D. *Langmuir* **1988**, *4*, 365. (k) Bain, C. D.; Troughton, E. B.; Tao, Y.-T.; Evall, J.; Whitesides, G. M.; Nuzzo, R. G. *J. Am. Chem. Soc.* **1989**, *111*, 321. (l) Ulman, A.; Eilers, J. E.; Tillman, N. *Langmuir* **1989**, *5*, 1147. (m) Whitesides, G. M.; Laibinis, P. E. *Langmuir* **1990**, *6*, 87.

S0002-7863(97)02717-0 CCC: $14.00

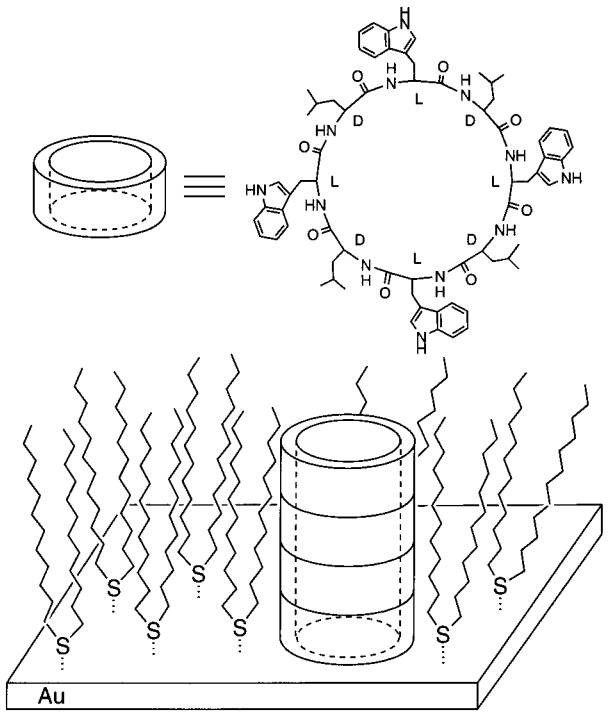

Figure 1. Schematic representation of a peptide cylinder embedded in the self-assembled monolayer of gold. The chemical structure of the cyclic peptide employed is shown in the flat ring-shaped conformation. The cyclic peptide subunit equipped with appropriate hydrophobic side chains can incorporate and self-assemble into tubular structures within the low dielectric constant environment of the lipid monolayer.

systems suitable for utilization in membrane mimetic studies such as molecular recognition,[8] catalysis,[9] and cellular interactions.[10] SAM supported membranes have also been exploited in the design of biosensors based on natural proteins, peptides, and ionophore structures.[11] We chose two SAMs based on 12-carbon chain thiols[7k,l] and thioethers[7j] which differ in their monolayer packing, orientation, and adhesion mode to the surface and examined their effectiveness in the formation of channeled monolayers.

(8) (a) Rickert, J.; Weiss, T.; Göpel, W. *Sens. Actuators, B* **1996**, *31* 45. (b) Huisman, B.-H.; Rudkevich, D. M.; van Veggel, F. C. J. M.; Reinhoudt, D. N. *J. Am. Chem. Soc.* **1996**, *118*, 3523. (c) Rickert, J.; Göpel, W.; Beck, W.; Jung, G.; Heiduschka, P. *Biosens. Bioelectron.* **1996**, *11*, 757. (d) Zhang, L.; Godinez, L. A.; Lu, T.; Gokel, G. W.; Kaifer, A. E. *Angew. Chem., Int. Ed. Engl.* **1995**, *34*, 235. (e) Motesharei, K.; Myles, D. C. *J. Am. Chem. Soc.* **1994**, *116*, 7413. (f) Schirebaum, K. D.; Weiss, T.; Thoden van Velzen, E. U.; Engbersen, J. F. J.; Reinhoudt, D. N.; Göpel, W. *Science* **1994**, *265*, 1413. (g) Willner, I.; Blonder, R.; Dagan, A. *J. Am. Chem. Soc.* **1994**, *116*, 9365. (h) Spinke, J.; Liley, M.; Guder, H.-J.; Angermaier, L.; Knoll, W. *Langmuir* **1993**, *9*, 1821. (i) Niwa, M.; Mori, T.; Nishio, E.; Nishimura, H.; Higashi, N. *J. Chem. Soc., Chem. Commun.* **1992**, 547. (j) Haussling, L.; Ringsdorf, H.; Schmitt, F.-J.; Knoll, W. *Langmuir* **1991**, *7*, 1837.

(9) (a) Motesharei, K.; Myles, D. C. *J. Am. Chem. Soc.* **1997**, *119*, 6674. (b) Willner, I.; Heleg-Shabati, V.; Blonder, R.; Katz, E.; Tao, G. *J. Am. Chem. Soc.* **1996**, *118*, 10321. (c) Willner, I.; Blonder, R.; Katz, E. *J. Am. Chem. Soc.* **1996**, *118*, 5310. (d) Zak, J.; Yuan, H.; Ho, M.; Woo, L. K.; Porter, M. D. *Langmuir* **1993**, *9*, 2772.

(10) (a) Margel, S.; Volger, E. A.; Firment, L.; Watt, T.; Haynie, S.; Sogah, D. Y. *J. Biomed. Mater. Res.* **1993**, *27*, 1463. (b) McConnell, H. M.; Watts, T. H.; Weis, R. M.; Brian, A. A. *Biochim. Biophys. Acta* **1986**, *864*, 95.

(11) (a) Cornell, B. A.; Braach-Maksvytis, V. L. B.; King, L. G.; Osman, P. D. J.; Raguse, B.; Wieczorek, L.; Pace, R. J. *Nature* **1997**, *387*, 580. (b) Boncheva, M.; Duschl, C.; Beck, W.; Jung, G.; Vogel, H. *Langmuir* **1996**, *12*, 5636. (c) Knichel, M.; Heiduschka, P.; Beck, W.; Jung, G.; Göpel, W. *Sens. Actuators, B* **1995**, *28*, 85. (d) Naumann, R.; Jonczyk, A.; Kopp, R.; van Esch, J.; Ringsdorf, H.; Knoll, W.; Graber, P. *Angew. Chem., Int. Ed. Engl.* **1995**, *34*, 2056. (e) Lang, H.; Koenig, B.; Vogel, H. *WO-B93/21528* **1992**. (f) Steinem, C.; Janshoff, A.; Galla, H.-J.; Sieber, M. *Bioelectrochem. Bioenerg.* **1997**, *42*, 213.

Results and Discussion

Formation of SAM-Supported Peptide Nanotubes. An eight-residue cyclic peptide with an alternating sequence of D-Leu and L-Trp residues was used in the present study. The cyclic peptide has been designed according to previously elaborated design principles with appropriate hydrophobic side chain moieties to facilitate its incorporation and self-assembly into the SAM surfaces (Figure 1).

Two methods for the incorporation of cyclic peptides into the monolayer systems have been investigated. In the first method (referred to hereafter as the stepwise method), the organosulfur monolayers were formed initially on gold films. These monolayers were then immersed in a solution of cyclic peptide in ethanol to allow peptide insertion into the monolayers and nanotube assembly on SAM surfaces (Figure 2A). In the second method (referred to hereafter as the coadsorbed method), the gold surfaces were immersed into a mixed ethanolic solution of cyclic peptide and either thiol or thioether adsorbates (Figure 2B). The self-assembly of the cyclic peptide subunits into tubular structures can in principle occur in either a perpendicular or parallel orientation with respect to the supporting gold surface. As shown in Figure 2, depending on the nature of the organosulfur employed and the method of the sample preparation, either orientation can be achieved.

The orientation of the SAM-supported self-assembled peptides onto tubes has been studied with grazing angle FTIR spectroscopy.[12] In grazing angle IR spectroscopy, the component of the electric-field vector of the polarized light parallel to the surface (*s*-polarized) is essentially inactive. However, the electric-field vector of the polarized light perpendicular to the surface (*p*-polarized) has a nonzero electric-field vector and hence is active. Considering that in the grazing angle infrared spectrum only vibrating bands with nonzero components in the perpendicular direction to the surface are active, the absorption of amide I and amide II bands of the cyclic peptides adsorbed on the surface can be used to analyze the orientation of the SAM-supported peptide nanotubes.

Previous IR studies[13] on peptides and proteins have shown the presence of two components for each amide I and II band, namely the perpendicular (⊥) and parallel (∥) components, with the amide I (⊥) and amide II (∥) being the stronger component in each band type. In general, for an antiparallel β-sheet structure the perpendicular component of the amide II band is either weak or absent. The presence of an amide I (⊥) band (C═O carbonyl stretching) and a strong N−H stretch in grazing angle IR spectra is indicative of the perpendicular orientation of the amide carbonyl group and the N−H bond to the surface—hence peptide nanotubes are laid perpendicular to the gold surface (Figure 3A). On the other hand, if the amide II (∥) band is most active with a weak amide I (∥) and N−H stretch, the self-assembled peptide nanotubes are oriented parallel to the gold surface (Figure 3B). In this setting, the components of the amide II (∥) band (out-of-phase combination of N−H in-plane bend and C−N stretch) are both perpendicular to the surface and hence are active. Furthermore, the position of the N−H stretch has been shown to be an indication of the intermolecular hydrogen bonding distance between the stacked peptide subunits and can be used to give an estimation of the intersubunit distances of the self-assembled tubular structures.

(12) (a) Crooks, R. M.; Xu, C.; Sun, L.; Hill, S. L.; Ricco, A. J. *Spectroscopy* **1993**, *8 (7)*, 28. (b) Porter, M. D. *Anal. Chem.* **1988**, *60*, 1143A. (c) Whitesell, J. K.; Chang, H. K. *Science* **1993**, *261*, 73.

(13) (a) Bandekar, J. *Biochim. Biophys. Acta* **1992**, *1120*, 123. (b) Krimm, S.; Bandekar, J. In *Advances in Protein Chemistry*; Anfinsen, C. B., Edsall, J. T., Richards, F. M., Eds.; Academic Press: Orlando, FL, 1986; pp 181−364. (c) Miyazawa T.; Blout, E. R. *J. Am. Chem. Soc.* **1961**, *83*, 712.

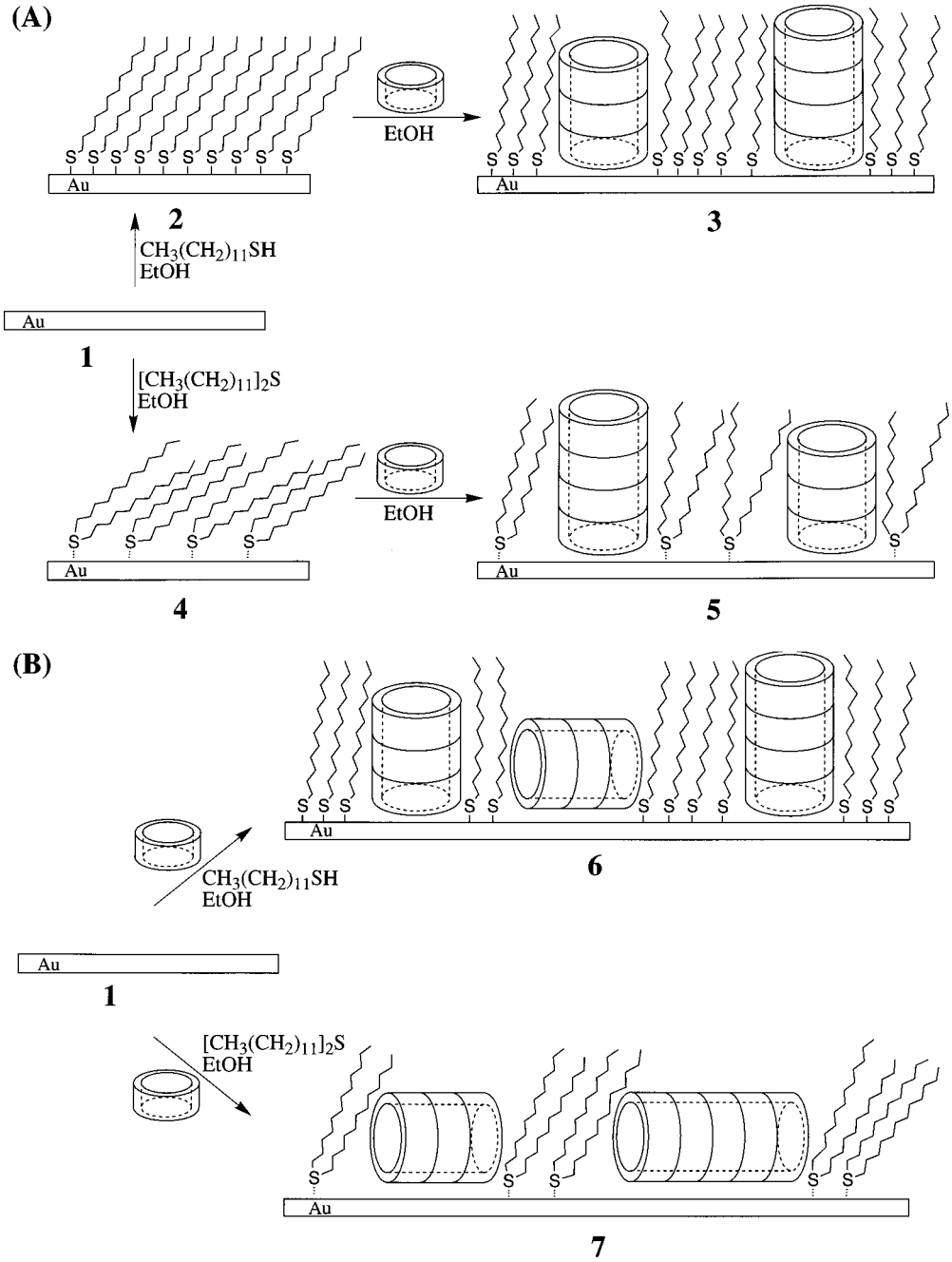

Figure 2. The orientation of SAM-supported peptide nanotubes can be controlled depending on the method of sample preparation. This figure schematically illustrates the formation of cyclic peptide incorporated monolayers via the stepwise (A) and the coadsorbed (B) methods for alkanethiol and thioether monolayers on gold. The stepwise method is shown to produce the desired perpendicularly oriented nanotubes on gold samples for both organosulfur monolayers. On the other hand, the coadsorbed method produces a small fraction of parallel oriented nanotubes for the thiolate monolayer and almost exclusively parallel oriented nanotubes for the thioether monolayer (see text for detailed discussion).

For all peptide incorporated monolayers, the N−H stretch at 3280 cm^{-1} corresponds to an intermolecular (N···O) distance of 2.8 to 2.9 Å regardless of the peptide orientation in the monolayers. This value is consistent with previous X-ray structures and electron diffraction analysis of self-assembled peptide nanotubes.[4,14]

The IR analysis (Figure 4) of thiolate monolayers for the stepwise method shows the predominate to exclusive presence of the amide I (⊥) band at 1635 cm^{-1} (Figure 4A), corresponding to the preponderance of tubular structures perpendicular to the plane of the gold surface. Moreover, the low intensity of amide I (∥) (1686 cm^{-1}) and amide II (∥) (1549 cm^{-1}) additionally supports the presence of perpendicular tubular structures. Similar results were also obtained for thioether monolayers in the stepwise method (Figure 4B). The monolayers from coadsorption of thiol and cyclic peptide show formation of a mixture of parallel and perpendicularly oriented tubes on gold film as indicated by the presence of an amide I (⊥) along with a medium intensity amide II (∥) band and amide I (∥) band (Figure 4C). The formation of tubular structures parallel to the gold surface is even more pronounced for the monolayers coadsorbed from thioether/cyclic peptide solutions from the predominate amide II (∥) and amide I (∥) bands (Figure 4D) and a very low intensity amide I (⊥) band. The formation of parallel nanotubes on the surface is presumed to be a

(14) (a) Ghadiri, M. R.; Kobayashi, K.; Granja, J. R.; Chadha, R. K.; McRee, D. E. *Angew. Chem., Int. Ed. Engl.* **1995**, *34*, 93. (b) Kobayashi, K.; Granja, J. R.; Ghadiri, M. R. *Angew. Chem., Int. Ed. Engl.* **1995**, *34*, 95.

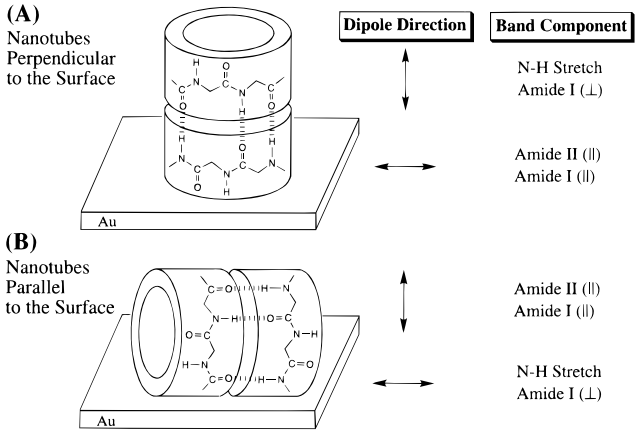

Figure 3. Grazing angle FTIR spectroscopy can be employed to estimate the orientation of the peptide nanotubes on solid surfaces by taking advantage of the orthogonal relationship between the amide I (⊥) and N−H stretch modes to that of the amide I (∥) and amide II (∥). Since in grazing angle IR spectroscopy only the perpendicular component of the incident light with respect to the plane of the surface is absorbed and hence detected, the presence of a strong amide I (⊥) band (C═O carbonyl stretching) and an intense N−H stretch are indicative of the perpendicular direction of the amide carbonyl group and the N−H bonds to the surface—hence peptide nanotubes are oriented perpendicularly to the gold surface (A). On the other hand, if the amide II (∥) band is most active with a along weak amide I (∥), the self-assembled peptide nanotubes are oriented parallel to the gold surface (B). In this setting, the components of the amide II (∥) bands (out-of-phase combination of N−H in-plane bend and C−N stretch) are both perpendicular to the surface and hence are active.

consequence of the competitive adsorption between the organosulfur compounds and the cyclic peptide to the gold surface. Due to the slower rate of adsorption of thioethers to gold compared to the thiols, a higher occurrence of parallel nanotubes on the surface has been observed for the thioether monolayers. Furthermore, the differences between thiols and thioethers with respect to their stability and monolayer packing order on gold may also be a significant contributor to the formation of oriented tubular structures.

Channel Activity of SAM-Supported Peptide Nanotubes. The ability of SAM-supported peptide nanotubes to function as size-selective ion channels was examined by cyclic voltammetry[15] by using three electroactive species of different sizes and charges: a negatively charged small redox active complex $[Fe(CN)_6]^{3-}$ that can travel through the 7.5 Å van der Waals radii cavity of the peptide channels, a positively charged small redox active complex $[Ru(NH_3)_6]^{3+}$ also small enough to pass through the cavity of the peptide channels, and a negatively charged redox complex $[Mo(CN)_8]^{4-}$ that is too large to enter the lumen of peptide channels. Cyclic voltammetry studies with these electroactive species also served to rule out the possibility of redox activity through monolayer defect sites.

As expected, the pure thiolate monolayers (**2**) showed virtually no redox activity for any of the above electroactive species, supporting the formation of well-packed monolayers (Figure 5).[16] Perpendicularly oriented SAM-supported self-assembled peptide nanotubes prepared via either the stepwise (**3**) or the coadsorbed method (**6**) showed redox activity for the two small electroactive species $[Fe(CN)_6]^{3-}$ and $[Ru(NH_3)_6]^{3+}$ that can traverse the channel lumen, but no activity when the larger ion $[Mo(CN)_8]^{4-}$ was used.[3j] The ion-channel activity for the thiolate monolayer is greater for the monolayers formed from the stepwise mechanism, as expected from the IR studies, due to formation of highly oriented perpendicular tubular structures. Selective channel activity was detected by observation of a single redox voltammogram corresponding to that of the $[Fe(CN)_6]^{3-}$ complex when a mixed redox solution containing equimolar amounts of $[Fe(CN)_6]^{3-}$ and $[Mo(CN)_8]^{4-}$ was used. Also as a control, thiolate monolayer samples soaked in pure ethanol overnight and then examined with the same redox complexes showed no noticeable difference in their redox voltammograms compared to the freshly prepared thiolate monolayers. This, in addition to the selective channel activity,

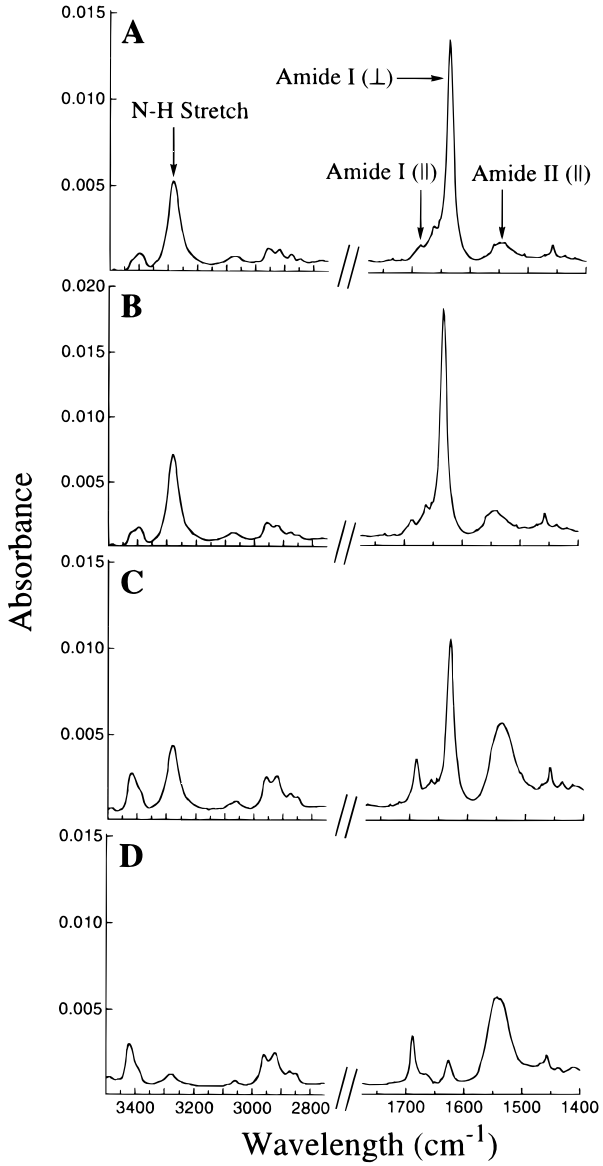

Figure 4. Grazing angle IR spectra of thiolate (A) and thioether (B) monolayers formed by the stepwise incorporation of cyclic peptides and thiolate (C) and thioether (D) formed by the coadsorbed incorporation of cyclic peptides on gold films. Note the strong amide I (⊥) band at 1635 cm^{-1} and also the absence of an amide II (∥) band at 1540 cm^{-1} in the nanotube incorporated stepwise monolayers (A and B) indicating their perpendicular orientation with respect to the gold surface. On the other hand, The strong amide II (∥)band at 1540 cm^{-1} and lack of amide I (⊥) band at 1635 cm^{-1} in the coadsorbed thioether monolayer (D) indicates the formation of parallel oriented peptide nanotubes on the gold surface. Spectrum C is indicative of a mixture of parallel and perpendicularly oriented peptide nanotubes.

(15) Bard, A. J.; Faulkner, L. R. *Electrochemical Methods: Fundamentals and Applications*; John Wiley & Sons: New York, 1980.

(16) (a) Chidsey, E. D.; Loiacono, D. N. *Langmuir* **1990**, *6*, 682. (b) Porter, M. D.; Bright, T. B.; Allara, D. L.; Chidsey, E. D. *J. Am. Chem. Soc.* **1987**, *109*, 3559. (c) Doblhofer, K.; Figura, J.; Fuhrhop, J.-H. *Langmuir* **1992**, *8*, 1811.

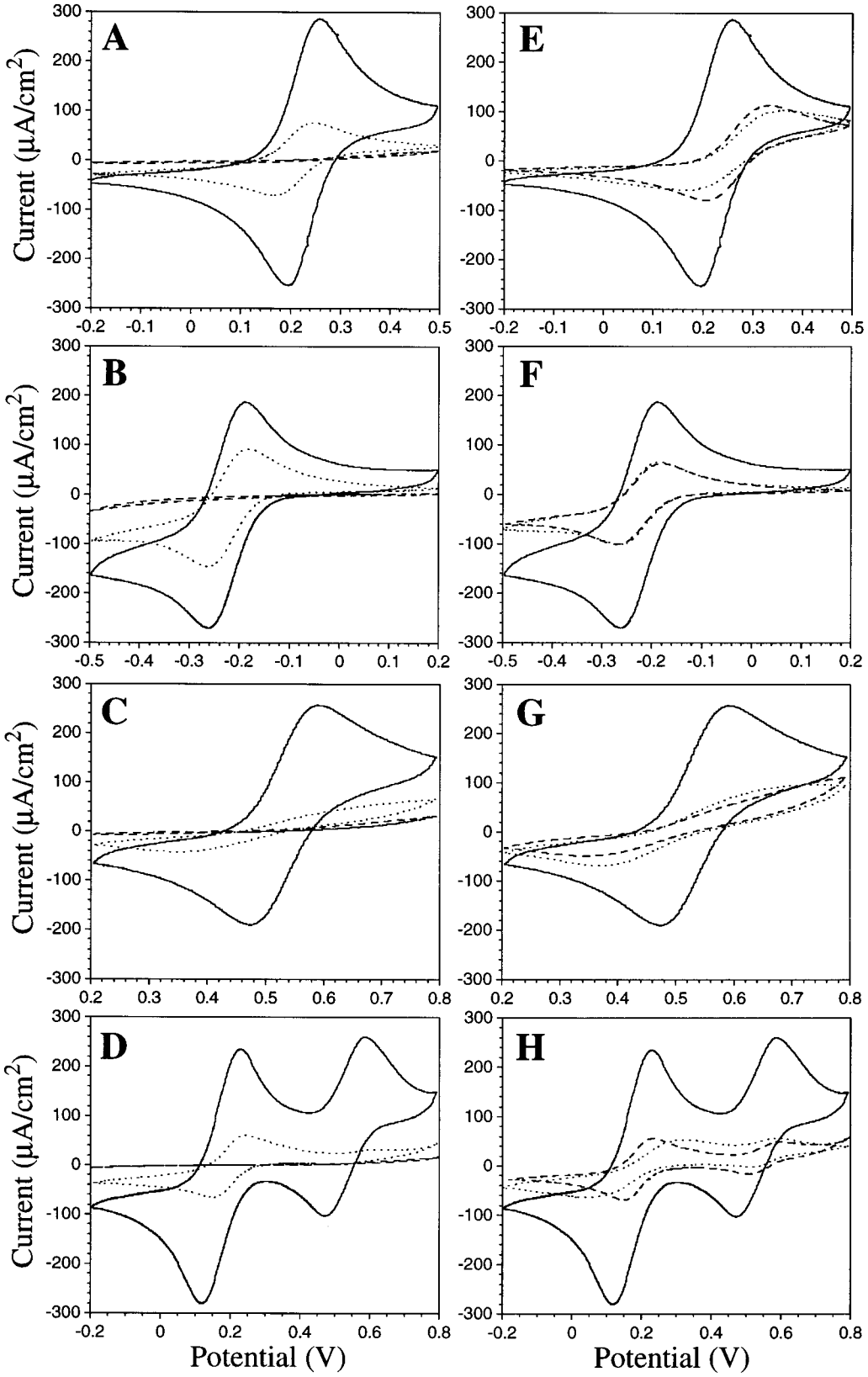

Figure 5. Cyclic voltammograms (— bare gold; - - - thiolate monolayer; and ··· samples prepared through the stepwise method) of thiolate monolayers in $K_3[Fe(CN)_6]$, $[Ru(NH_3)_6]Cl_3$, $K_4[Mo(CN)_8]$, and $K_3[Fe(CN)_6]/K_4[Mo(CN)_8]$ mixed analyte solutions (A, B, C, and D, respectively). Also, the cyclic voltammograms of thioether monolayers (— bare gold; - - - thioether monolayer; and ··· samples prepared through the coadsorbed method) in the same electroactive solutions (E, F, G, and H, respectively) . The voltammograms for samples prepared through the coadsorbed method for thiolate monolayers and those prepared through the stepwise method for thioether monolayers are not shown.

is an indication that the redox voltammograms observed are due to channel formation by cyclic peptides and not to monolayer destruction during the incorporation of the peptides by ethanol and desorption of thiolates from the surface.

As expected, the pure thioether monolayers (**4**) showed a small amount of redox activity for all electroactive species due to their less-well-packed monolayer structure and their lower insulating character. The thioether monolayers, after being

immersed in the cyclic peptide solution overnight (**5**), were shown to form tubes perpendicular to the surface by IR spectroscopy, indicating the formation of channels. However, these monolayers consistently showed a smaller redox voltammogram for all the electroactive species compared to that of the pure thioether monolayers. We hypothesize that the lower redox activity in the voltammograms of the peptide channels is due to a better packing and somewhat increased thickness of the thioether monolayers as a consequence of peptide incorporation. Assembly of the more rigid peptide tubes in the flexible monolayer of thioethers is expected to cause a rearrangement of the thioether adsorbates to form a more densely packed monolayer in which the adsorbates align themselves with the tubes and hence reduce the defect sites and nominally increase the thickness of the monolayer. Further evidence for the formation of channels in these thioether monolayers comes from their cyclic voltammograms obtained in a mixed $[Fe(CN)_6]^{3-}$ and $[Mo(CN)_8]^{4-}$ solution. Although the pure thioether monolayers do not show any selectivity for the two redox complexes, the channel incorporated monolayers (**5**) do show selective redox activity for the smaller $[Fe(CN)_6]^{3-}$ complex, which is attributed to the presence of peptide channels and not defect sites. As expected, for the parallel oriented self-assembled peptide nanotubes that are formed by the coadsorption method (**7**) no channeling effect was observed.

Impedance spectroscopy[17] was also used to document the transport activity of SAM-supported peptide nanotubes on gold by monitoring the capacitance of the monolayers in the double-layer matrix in 10 mM $Ca(NO_3)_2$ solution.[18] In general, a decrease in the thickness of the monolayer or an increase in the dielectric constant of the monolayer increases the monolayer capacitance.[11c,19] In our studies, however, the changes in capacitance due to changes in monolayer thickness are minimal and hence the observed changes are a direct consequence of the presence of cyclic peptide nanotubes and the resulting ion flux through the channels. Analysis of the impedance measurements was carried out by comparing the experimental data with model electrical equivalent circuits where elements in the model equivalent circuit are assigned to actual components in the system. In the analysis of our systems, we have assumed a simple model for a fitting procedure corresponding to a solution resistance of 282 Ω in series with a parallel resistor/capacitor that corresponds to the membrane. From such analyses, the capacitance of a gold sample (Figure 6) in 10 mM $Ca(NO_3)_2$ was estimated and shown experimentally to be 33.92 μF/cm^2. Similar measurements for thiolate and thioether monolayers were 1.06, and 1.22 μF/cm^2, respectively. These measurements are in close agreement with previously published values for monolayers of similar thickness and structure independent of the analyte solution and applied potential.[20] The observed increase in the capacitance (Table 1) of the monolayers incorporated with the cyclic peptide channels compared to the pure monolayers is a consequence of the penetration of ions through the channels (**3**, **5**, and **6**). A slight increase in the capacitance was also observed for the coadsorbed monolayers of thioether and cyclic peptides (**7**). Although channel formation is unlikely (because of the parallel orientation of peptide nanotubes), the possibility of a higher concentration of ions trapped in the parallel tubes on the surface is sufficient to increase the dielectric difference of the double-layer system and hence increase the monolayer capacitance.

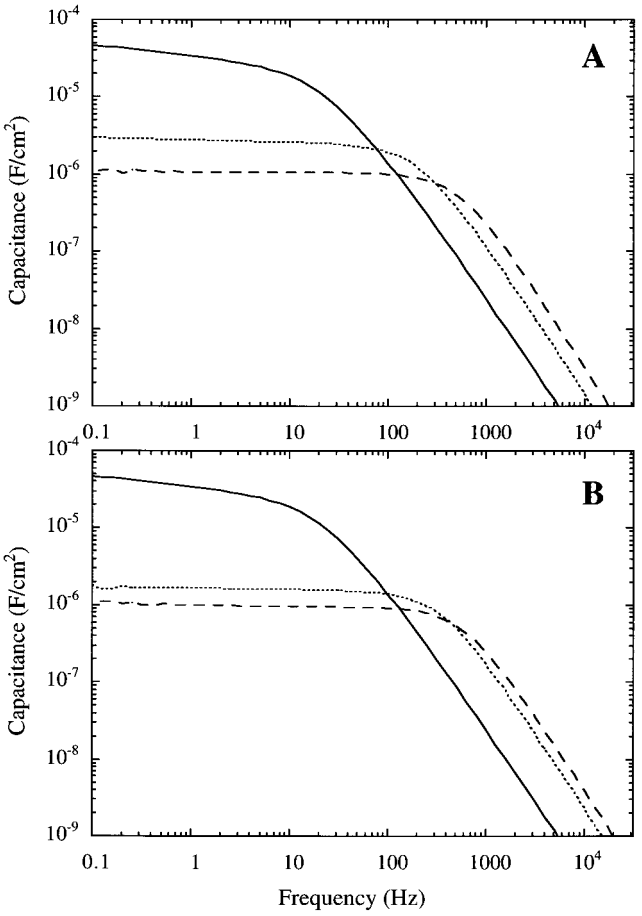

Figure 6. Capacitance plots (— bare gold; - - - thiolate monolayer; and ··· samples prepared through stepwise method) of thiolate monolayers (A) and (— bare gold; - - - thioether monolayer; and ··· samples prepared through coadsorbed method) thioether monolayers (B) in 10 mM $Ca(NO_3)_2$. The capacitance for samples prepared through the coadsorbed method for thiolate monolayers and those prepared through the stepwise method for thioether monolayers are not shown.

Table 1. Major Peptide IR Bands and Capacitance Values for the Substrate Surfaces Examined

	IR[b] (cm^{-1})				
substrate surfaces[a]	amide I (⊥)	amide I (∥)	amide II (∥)	N−H stretch	capacitance[c] (μF/cm^2)
1					33.92
2					1.06
3	1635 (vs)	1686 (vw)	1549 (vw)	3282 (s)	1.22
4					0.98
5	1633 (vs)	1686 (vw)	1541 (vw)	3278 (s)	1.94
6	1630 (s)	1687 (w)	1541 (m)	3278 (s)	1.34
7	1628 (vw)	1689 (w)	1543 (m)	3280 (vw)	1.61

[a] See Figure 2 for substrate surface numbering. [b] Relative IR band intensities: very strong (vs), strong (s), medium (m), weak (w), very weak (vw). [c] In 10 mM $Ca(NO_3)_2$ analyte solution.

Conclusion

In summary, we have described the design, synthesis, and characterization of a novel diffusion-limited size-selective ion sensor based on the self-assembly of flat ring-shaped cyclic peptides into tubular channels in the organosulfur self-assembled monolayers on gold films. Variations in the cyclic peptide diameter and their channeling selectivity toward different

(17) (a) Macdonald, J. R., Ed. *Impedance Spectroscopy*; John Wiley & Sons: New York, 1987. (b) Janshoff, A.; Wegener, J.; Steinem, C.; Sieber, M.; Galla, H.-J. *Acta Biochim. Pol.* **1996**, *43*, 339.

(18) Sindholm-Sethson, B. *Langmuir* **1996**, *12*, 3305.

(19) Gafni, Y.; Weizman, H.; Libman, J.; Shanzer, A.; Rubinstein, I. *Chem. Eur. J.* **1996**, *2*, 759.

(20) (a) Plant, A. L.; Gueguetchkeri, M.; Yap, W. *Biophys. J.* **1994**, *67*, 1126. (b) Steinem, C.; Janshoff, A.; Ulrich, W.-P.; Sieber, M.; Galla, H.-J. *Biochim. Biophys. Acta* **1996**, *1279*, 169.

species, along with the differences in the chain length of the organosulfur adsorbates, are expected to increase the repertoire of the sensor applications.

Experimental Section

General Methods. All reagents were of highest purity and purchased from Aldrich Chemical Company, Inc. and were used without further purification unless otherwise noted. All solvents were purchased from Fisher Scientific (HPLC Grade). The amino acid units of peptide were purchased from Nova Biochem (San Diego, CA). The cyclic peptide was synthesized, purified, and characterized as previously reported.[21]

Preparation of Gold Substrate. Gold samples were prepared by thermal evaporation of gold (1000 Å) on silicon wafers (Silicon Sense, Inc. Nashua, NH) precoated with 100 Å of chromium at 4×10^{-6} Torr. The silicon wafers, prior to evaporation, were soaked in a 3:1 H_2SO_4/H_2O_2 (30%) solution and then rinsed extensively with deionized water and ethanol. The thickness of the deposited metallic films during the evaporation was measured by the changes in the frequency of oscillation of a quartz crystal.

Preparation of Monolayer Samples. (a) The Stepwise Procedure. The gold-coated silicon wafers were immersed in 10 mM ethanolic solutions of 1-dodecanethiol or dodecyl sulfide for a minimum of 12 h. The resulting organosulfur monolayers were then rinsed with ethanol and immersed in 0.1 mM solutions of cyclic peptide in ethanol for 12 h.

(b) The Coadsorbed Procedure. The gold-coated silicon wafers were immersed in a mixed solution containing 0.1 mM cyclic peptide and 10 mM of either organosulfur adsorbate for 12 h. All samples were rinsed with ethanol and dried under a stream of argon prior to analysis.

Grazing Angle Infrared Spectroscopy. FTIR data were obtained by using a Nicolet 550 Magna Series II instrument equipped with a narrow band liquid nitrogen cooled MCT detector and a Spectra Tech (Stamford, CT) grazing angle attachment. Grazing angle spectra of monolayer samples in nitrogen atmosphere were obtained by using 800 scans at 4-cm^{-1} resolution with *p*-polarized light at an 80° angle of incident. The spectra were analyzed with the Omnic 3.0 software package (Nicolet).

Cyclic Voltammetry. Cyclic voltammograms were obtained by using a Bioanalytical Systems, Inc. (Lafayette, IN) CV-27 potentiostat. A standard three-electrode configuration was used with the monolayer sample on gold film as the working electrode, SCE as the reference electrode, and a platinum wire as the auxiliary electrode in a well-shaped Teflon cell. The area of the gold sample exposed to electrolyte was 0.24 cm^2. The redox regents used were 1 mM $K_3[Fe(CN)_6]$ or $[Ru(NH_3)_6]Cl_3$ in 1 M KCl analyte solution. Cyclic voltammetry with 1 mM $K_4[Mo(CN)_8]$[22] was performed in 0.1 M acetate buffer (pH 5.65). The scan rate for all measurements was set at 50 $mV \cdot s^{-1}$. The voltammograms were recorded and analyzed with the Igor Pro 3.0 software package (Lake Oswego, OR).

Impedance Spectroscopy. Impedance and capacitance measurements were carried out in the frequency range of 32 kHz to 0.1 Hz with an amplitude of 50 mV and fixed static potential of zero volt with a Solartron SI-1260 frequency response analyzer. The measurements were performed in a well-shaped Teflon cell with 10 mM $Ca(NO_3)_2$ (supporting electrolyte only) and platinum wire as the auxiliary electrode. The area of the gold sample exposed to electrolyte was 0.24 cm^2. The results were presented as Bode plots and analyzed with a ZView software package (Solartron) based on complex nonlinear least-squares (CNLS) fitting (LEVM6)[23] to an equivalent circuit consisting of a resistor in series with a parallel capacitor/resistor combination that corresponds to the membrane.

Acknowledgment. We thank C. Choi for peptide synthesis and H. S. Kim for providing the initial sample of the cyclic peptide. We also thank M. J. Sailor and M. A. Case for helpful discussions. K.M. acknowledges the National Institutes of Health for a postdoctoral fellowship (GM18309). This work is supported by the Office of Naval Research (N000149511293) through the Multi-Disciplinary University Research Initiative (MURI-95) of the Department of Defense.

JA9727171

(21) Hartgerink, J. D.; Granja, J. R.; Milligan, R. A.; Ghadiri, M. R. *J. Am. Chem. Soc.* **1996**, *118*, 43.

(22) For a procedure to synthesize this compound see: van de Poel, J.; Neumann, H. M. *Inorg. Synth.* **1968**, *11*, 53.

(23) See page 180 of ref 17a.